The Length of a Single Turn Controls the Overall Folding Rate of "Three-Fingered" Snake Toxins†

Margherita Ruoppolo,‡,§ Mireille Moutiez,|| Maria Fiorella Mazzeo,‡ Piero Pucci,§,⊥,# André Ménez,|| Gennaro Marino,§,⊥,# and Eric Quéméneur*,||

Dipartimento di Chimica, Università degli Studi di Salerno, Salerno, Italy, Centro Internazionale di Servizi di Spettrometria di Massa, CNR, Università di Napoli "Federico II", Napoli, Italy, CEA, Département d'Ingénierie et d'Etudes des Protéines, C. E. Saclay, France, Dipartimento di Chimica Organica e Biologica, Università di Napoli "Federico II", Napoli, Italy, and CEINGE, Biotecnologie Avanzate, scrl, Napoli, Italy

Received June 23, 1998; Revised Manuscript Received September 2, 1998

ABSTRACT: Snake curaremimetic toxins are short all-β proteins, containing several disulfide bonds which largely contribute to their stability. The four disulfides present in snake toxins make a "disulfide β-cross"-fold that was suggested to be a good protein folding template. Previous studies on the refolding of snake toxins (Ménez, A. et al. (1980) *Biochemistry 19*, 4166−4172) showed that this set of natural homologous proteins displays different rates of refolding. These studies suggested that the observed different rates could be correlated to the length of turn 2, one out of five turns present in the toxins structure and close to the "disulfide β-cross". To demonstrate this hypothesis, we studied the refolding pathways and kinetics of two natural isotoxins, toxin α (*Naja nigricollis*) and erabutoxin b (*Laticauda semifasciata*), and two synthetic homologues, the α mutants, α60 and α62. These mutants were designed to probe the peculiar role of the turn 2 on the refolding process by deletion or insertion of one residue in the turn length that reproduced the natural heterogeneity at that locus. The refolding was studied by electrospray mass spectrometry (ESMS) time-course analysis. This analysis permitted both the identification and quantitation of the population of intermediates present during the process. All toxins were shown to share the same sequential scheme for disulfide bond formation despite large differences in their refolding rates. The results presented here demonstrate definitely that no residues except those forming turn 2 accounted for the observed differences in the refolding rate of toxins.

Proteins that are structurally related to snake curaremimetic toxins are good examples of short all-β proteins, containing several disulfide bonds which largely contribute to their stability. The four disulfides present in snake toxins make a "disulfide β-cross"-fold that was suggested to be a good protein folding template (*1*). The fold consists of five strands forming 3 loops owing to disulfide bridges (Figure 1A). Such a structure is adopted by many proteins with unrelated functions: nicotinic and muscarinic acetylcholine receptor, an acetylcholine esterase inhibitor (fascicullin), cardiotoxins, a calcium-channel ligand (calciceptine), an inhibitor of platelet aggregation (for a review, see ref *2*), and the activator of complement CD59 (*3*, *4*). The site responsible for the interaction of erabutoxin Ea with the nicotinic acetylcholine receptor was demonstrated to be borne by the bottom of the 3 loops by site-directed mutagenesis (*5*).

Very little information is available on the refolding of snake toxins in vitro. Early studies provided an original example of a natural set of homologous proteins displaying different rates of refolding (*6*). In particular, toxin α from *Naja nigricollis*, 61 residues, and erabutoxin b (Eb)[1] from *Laticauda semifasciata*, 62 residues, showed a very large difference in their rate of oxidative refolding (*6*). The sequences of toxin α and Eb differ for 17 residues out of a total of 62 (Figure 1B), and many residues might account for this discrepancy. Schematically, sequence variations are located within four regions of the protein: 4 out of 6 and 5 out of 7 residues differ in the N- and C-terminal portions, respectively, whereas 6 substitutions occur in the segment 22−32 encompassing strand 3 (S3). Moreover, turn 2 connecting loops 1 and 2 is one amino acid longer in Eb

† The work was supported by EC Grant BIO4-CT96-0436 to G.M. and E.Q. and by Progetto Strategico Biologia Strutturale, CNR, and PRIN, Biologia Strutturale, MURST, Rome, Italy.

* To whom correspondence should be addressed at CEA-DIEP, Bâtiment 152, C. E. Saclay, F-91191 Gif-sur-Yvette, France. Telephone: (33) 1-6908-7648. Fax: (33) 1-6908-9137. E-mail: eric.quemeneur@cea.fr.

‡ Università degli Studi di Salerno.

§ Centro Internazionale di Servizi di Spettrometria di Massa, Università di Napoli "Federico II".

|| CEA.

⊥ Dipartimento di Chimica Organica e Biologica, Università di Napoli "Federico II".

CEINGE.

[1] Abbreviations: AChR, nicotinic acetylcholine receptor; CAM, carboxyamidomethyl group; DTT, reduced dithiothreitol; EDTA, ethylenediamine tetraacetic acid; Eb, erabutoxin b from *Laticauda semifasciata;* ESMS, electrospray mass spectrometry; GSH, reduced glutathione; GSSG, oxidized glutathione; HPLC, high-performance liquid chromatography; IAM, iodoacetamide; MALDIMS, matrix-assisted laser desorption ionization mass spectrometry; RNase A, ribonuclease A; α, natural toxin α from *Naja nigricollis*; α60, α61, α62, synthetic variants of toxin α varying in length from 60 to 62 residues.

10.1021/bi981492j CCC: $15.00
Published on Web 10/26/1998

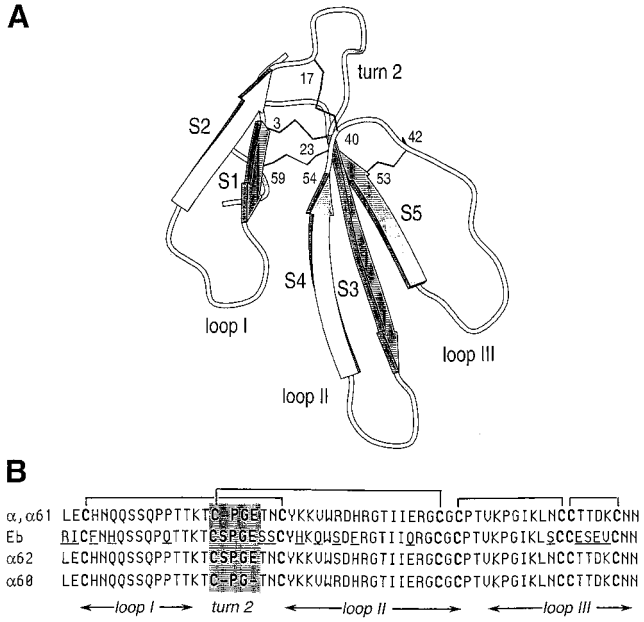

FIGURE 1: (A) Ribbon structure of toxin α from *Naja nigricollis* (drawn using MOLSCRIPT, (*30*)). The 8 cysteine side chains are drawn as lines and numbered. β-strands are numbered from S1 to S5. Turn 2 is at the top of the molecule close to the disulfide knot. (B) Sequence alignment of neurotoxins and their variants used in this study. Residues that differ between toxin α and erabutoxin b are underlined. α61 is a synthetic analogue of toxin α, and α60 and α62 are synthetic variants. The sequence of turn 2 is shaded.

(from 4 to 5 residues). There is no easy correlation between these variations in sequence and structural changes. Amino acid substitutions taking place in different sites of the toxins sequences affect their overall structures to various extents. Wu et al. (*7*) reported the structural role of Leu1 in cardiotoxin II, a structurally related family of toxins: its change to a D-Leu or a Gly had a significant effect on the secondary structure content of the protein. On the contrary, the CD spectra of toxin α and Eb superimposed perfectly (*6*) despite the substitution of Leu-Glu to Arg-Ile at the N-terminus. This suggests that the effects of these variations are compensated at a different region of the protein, most likely at the close C-terminus.

It is even more difficult to correlate variations in the sequence of toxins to differences in the rates of refolding. The above quoted studies suggested that the possible determinants of these observed different rates arise from sequence variations in some secondary structure elements, particularly turn 2 that could affect important steps in the folding process. However, such a hypothesis could not be proved at that time as the results obtained suffered for limits in the experimental conditions: (i) refolding was performed by air oxidation, in the absence of a redox buffer, leading to an accumulation of non-productive intermediates; (ii) the sequences of the proteins studied differed in many positions other than turn 2; and (iii) circular dichroism used to monitor the appearance of native toxin provided only an average measurement of the rate of secondary structure formation, without description of the folding pathways.

The interest in the "three-fingers"-fold in protein engineering (*8, 9*) has motivated the re-examination of previous studies taking advantage of recent developments in mass spectrometry and peptide synthesis. The introduction of mass spectrometry has allowed a great progress in our understanding of the folding pathways of denatured proteins either with intact native disulfide bonds (*10*) or with reduced ones (*11*−*13*). In the latter case the determination of the chemical nature and the time-course analysis of refolding intermediates permitted the unambiguous determination of the kinetic role of disulfide bond formation in the refolding process.

In this paper, we used mass spectrometry to study the folding pathways and the kinetics of refolding of snake toxins. Experiments were performed in the presence of reduced and oxidized glutathione in order to avoid the accumulation of irreversibly trapped off pathway intermediates and to enhance rate-limiting isomerizations. The refolding of two homologous toxins, toxin α and Eb, from the set previously studied by Ménez et al. (*6*) was undertaken to determine their pathways and rates of folding in the presence of glutathione. Furthermore, the specific role of turn 2 in the kinetic control of the refolding of these proteins was investigated using synthetic mutants of snake toxin α. Two variants, α60 and α62, were synthesized with the goal of getting rid of any possible interference from other amino acid substitutions in the sequence. Variant α62 has an insertion in turn 2 as observed in Eb and other toxins (*2*), whereas α60 derives from *Astrotia stokesii* toxin A which displays a deletion in this turn. Toxin A was shown to refold faster than toxin α (*6*).

The results presented in this paper show that all toxins share the same sequential pathway for disulfide bond formation despite large differences in their refolding rates and no residues except those forming turn 2 account for the observed differences in their refolding rates.

MATERIALS AND METHODS

Natural toxin α was prepared from the venom of *N. nigricollis* (Institut Pasteur, France) by the procedure of Eaker and Porath (*14*) and was tritium-labeled according to Ménez et al. (*15*) and Charpentier et al. (*16*). Erabutoxin b was purified from *L. semifasciata* according to Sato and Tamiya (*17*).

Synthetic toxins α60, α61, and α62 were prepared by solid-phase peptide synthesis on a Applied Biosystems 431A synthesizer, using the Fmoc strategy. Fmoc-Asp(Rink amide MBHA resin)-OtBu (0.45 mmol/g) was from Novabiochem. Amino acid protecting groups were as follows: OtBu (Glu, Asp), trityl (Cys, His, Asn, Gln), tBu (Ser, Thr, Tyr), Boc (Lys, Trp), and Pmc (Arg). Cleavage of the proteins from the resin and simultaneous deprotection of the side chains were achieved by treatment with trifluoroacetic acid/triisopropylsilane/H_2O (9:0.5:0.5) for 30 min at room temperature. The crude proteins were washed 3 times with ether and solubilized in 10% acetic acid. They were then lyophilized and purified by HPLC using a C18−5μ Bondasorb column in the following conditions: solvent A (H_2O, TFA 0.1%), solvent B (acetonitrile); 0%−21% B (5 min), 21%−25% B (20 min), 25%−80% B (5 min).

The concentration of solutions of natural and synthetic toxins was determined using a molar extinction coefficient of 6490 M^{-1} cm^{-1} at 280 nm (*6*).

Peptide Mapping of Synthetic Toxins. All the toxins were reduced and denatured with a 50-fold molar excess of DTT (mol DTT/mol SH) in 0.1 M Tris-HCl, 1 mM EDTA, pH

8.5, containing 6 M guanidinium chloride, for 2 h at 37 °C under nitrogen atmosphere. After reduction and denaturation, the proteins were carboxyamidomethylated with iodoacetamide (IAM mol/SH mol = 10:1) for 5 min at room temperature in the dark. The excess of reagents was then removed by HPLC desalting using a Vydac 218TP54 reversed-phase C18 column (0.46 cm × 25 cm). The elution system consisted of 0.1% TFA in water (solvent A) and 0.07% TFA in 95% acetonitrile/5% water (solvent B). Samples were purified from the excess of reagents with a linear gradient of solvent B from 5% to 95% at flow rate of 1 mL/min. Eluted proteins were monitored at 220 nm. The protein fraction was recovered and lyophilized. Tryptic digestion was performed in 0.4% ammonium bicarbonate, pH 8.5, at 37 °C for 4 h, using an enzyme/substrate ratio of 1:50 (w/w). MALDI analysis was carried out using a PerSeptive Biosystem Voyager DE instrument mass spectrometer. The mass range was calibrated using insulin (5734.5 Da) as internal standard. Samples were dissolved in 0.1% TFA at a 50 pmol/μL concentration; 1 μL was applied to a sample slide and allowed to air-dry before applying 1 μL of a solution of a cyano-4-hydroxycinnamic acid in ethanol/CH_3CN/0.1% TFA (1:1:1) (10 mg/mL). The matrix was allowed to air-dry before collecting spectra.

Refolding Reactions. The toxin samples were reduced and denatured as described above. The protein solution was then separated from the excess of DTT and denaturant by HPLC desalting. The protein fraction was recovered, lyophilized, and used within 2 days. Reduced and oxidized glutathione stock solutions were made fresh daily in 0.1 M Tris-HCl (pH 7.5) at a concentration of 25 mM; 1 mM EDTA was added to the buffers to prevent oxidation of SH groups catalyzed by traces of heavy metals.

Lyophilized, reduced, and denatured toxins were dissolved to a concentration of approximately 50 μM in 1% CH_3COOH and then diluted into the refolding buffer (0.1 M Tris-HCl, 1 mM EDTA, pH 7.5) to a final concentration of 15 μM. The desired amounts of GSH and GSSG stock solutions were added to initiate refolding; typically, final concentrations of the glutathione species were 3 mM GSH/0.3 mM GSSG. The pH of the solution was adjusted to 7.5 with Tris-base and the reaction carried out at 25 °C under nitrogen atmosphere. Each set of data was obtained as the mean of two independent folding experiments. A 4% difference in the ion current of individual components detected in the refolding experiments performed completely independently of each other was obtained.

Alkylation of the Refolding Aliquots. The refolding was monitored on a time-course basis by sampling aliquots of the refolding mixture at appropriate intervals. The protein samples were alkylated under conditions developed to prevent reshuffling of S−S bonds (*11*, *18*). IAM was freshly dissolved in 0.1 M Tris-HCl, containing 1 mM EDTA (pH 7.5) at 65 °C and cooled to room temperature before use. During preparation of the reagents, the solutions were protected from light to minimize photolytic production of iodine which is a very potent oxidizing agent for thiols. The refolding aliquots (100 μL) were added to an equal volume of a 2.2 M IAM solution. Alkylation was performed for 30 s, in the dark, at room temperature, under nitrogen atmosphere. After 30 s, 50 μL of 5% TFA was added, and the aliquots were quickly vortexed and desalted by HPLC as described above. The eluted protein fraction was recovered and lyophilized.

Electrospray Mass Analysis. ESMS analyses were carried out using a BIO-Q triple quadrupole mass spectrometer equipped with an electrospray ion source (Micromass). The protein samples were dissolved in H_2O containing 2% CH_3COOH and diluted 1:1 with CH_3CN; 10 μL (10−20 pmol/μL) was introduced into the ion source via loop injection at a flow rate of 10 μL/min. Spectra were recorded by scanning the quadrupole at 10 s/scan. Data were acquired and elaborated by the MassLynx software. Each population of intermediates was accurately quantified by measuring the total ion current produced by each species (*12*, *13*). Mass-scale calibration was performed by means of multiply charged ions from a separate injection of horse heart myoglobin (average molecular mass 16951.5 Da).

Binding Studies. Monoclonal antibody Mα-1 (*19*) was kindly provided by J.-C. Boulain. Radiobinding assays were performed with Mα-1 using [^{3}H]-toxin α. Varying amounts of toxins were incubated overnight at 4 °C with Mα-1 (9.4 nM), [^{3}H]-toxin α (10 nM), and 6.25% normal horse serum in PBS 100 mM 0.5% BSA, pH 7.0. PEG 6000 (final concentration: 12.5% (w/v)) was then added to the solutions that were stirred and centrifuged at 10000*g* for 25 min. The pellets were dissolved in 750 μL of 0.05 N NaOH and 10 mL of scintillation solution (Aqualuma). The radioactivity was counted on a Rackbeta counter (LKB).

The acetylcholine receptor (AChR) from the electric organ tissue of *Torpedo marmorata* was prepared as described by Sobel et al. (*20*). Competition experiments made with AChR were performed at equilibrium, using [^{3}H]-labeled toxin as a radioactive tracer. Varying amounts of native toxins were incubated with AChR (2 nM) and [^{3}H]-toxin α (27 Ci/mmol, 10 nM) for 18 h at 20 °C, and the mixture was filtered through Millipore filters (HAWP) which had been soaked in PBS 0.01% Triton buffer. The filters were washed with 10 mL of PBS 0.01% Triton buffer, dried, and, after addition of 10 mL of scintillation solution (Lipoluma), counted as previously described. Equilibrium dissociation constants were determined from competition experiments according to Cheng and Prusoff (*21*).

The amount of native toxin in the refolding mixture could be determined for each mutant and at each time point using the competition data previously obtained. Refolding samples were incubated with AChR and [^{3}H]-toxin α as described above. The final concentrations of protein tested were 4×10^{-8} and 1×10^{-7} M. These concentrations displace respectively 90% and 100% of the labeled ligand when the native toxin is used. The percentage of active toxin was deduced from comparison with the standard competition curves.

RESULTS

The tridimensional structure of the class of toxins under study is essentially maintained by the four disulfide bonds which act as bolts. Reduction of these bridges is sufficient to abolish secondary structure for both toxin α and Eb (as shown by CD analysis), but it is not sufficient to abolish all tridimensional interactions since reduced toxins refold in a few minutes compared to reduced and denatured ones (data not shown). In this report, all experiments were performed

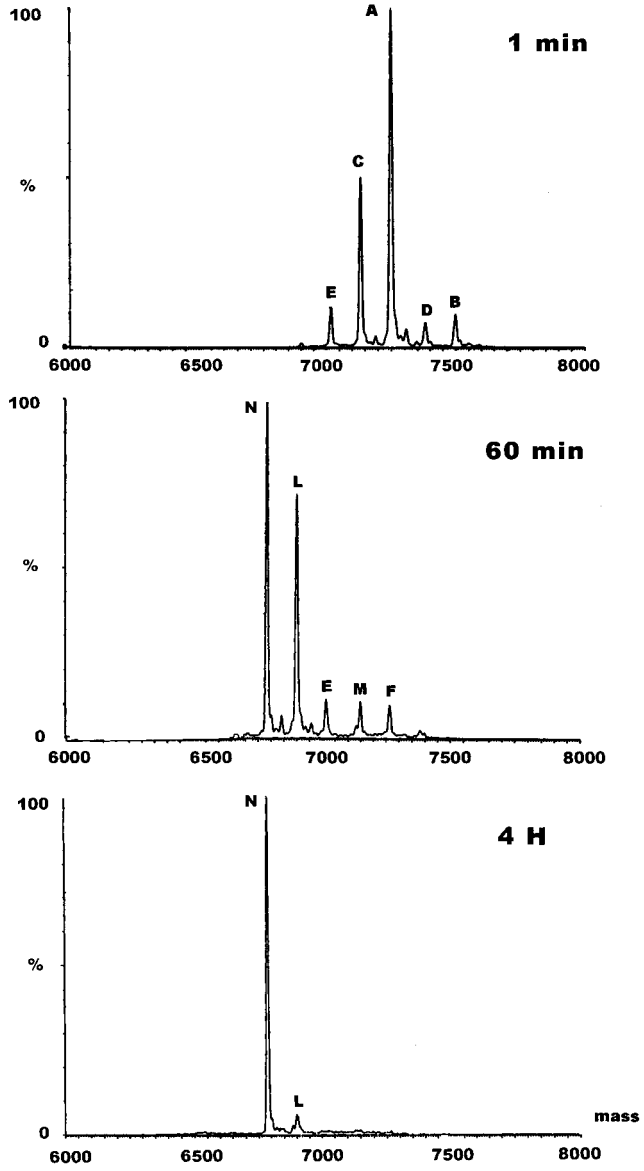

FIGURE 2: Electrospray mass spectrometric analysis of aliquots of the refolding mixture of natural toxin α in the presence of 3 mM GSH and 0.3 mM GSSG withdrawn at time 1 min (A), 60 min (B), and 4 h (C) and alkylated with 1.1 M IAM.

with proteins denatured and reduced in the presence of 6 M guanidinium chloride and DTT as described in Materials and Methods. The reduced and denatured proteins were then incubated in the presence of 3 mM GSH/0.3 mM GSSG for oxidative refolding. These redox conditions were chosen to mimic the concentrations of GSH and GSSG within the lumen of the endoplasmic reticulum (*22*), the site at which native disulfide bonds form during biosynthesis. Aliquots of the refolding process were withdrawn at different time intervals, trapped by alkylation of the free thiols, and analyzed by ESMS to identify the disulfide bonded intermediates formed. The carboxyamidomethylation reaction used to trap the free SH groups increased the molecular mass of the intermediates by a fixed amount, 57 Da for each free SH group, allowing the separation by mass of intermediates containing different numbers of disulfide bonds and the determination of their relative concentration during the refolding (*11*−*13*).

Refolding of Natural Toxins. Figure 2 shows the deconvoluted ESMS spectra of the samples withdrawn at 1 min (A), 60 min (B), and 4 h (C) of the refolding of the natural toxin α. At different times, different populations of disulfide intermediates are present which were identified on the basis of their accurate molecular mass. The measured molecular masses, the expected mass values, and the identification of the various intermediates are shown in Table 1. Each population of trapped intermediates is characterized by a different number of intramolecular disulfide bonds (indicated as *n*S in Table 1), mixed disulfides with the exogenous glutathione (*n*G), and carboxyamidomethyl groups (*n*CAM). The number of CAM groups corresponds to the number of free thiols present in the refolding intermediates, and it is therefore indicated as *n*H. It is important to emphasize that each observed molecular mass corresponds to a population of isomers, in which the total number of disulfides, free thiols, and protein-SSG mixed disulfides is defined, whereas the positions of the effective cysteine residues involved are not identified. The number of possible isomers within each population is indicated in Table 1.

Table 1: ESMS Analysis of the Intermediates Formed in the Refolding of Natural Toxin α

component	measured MW (Da)	identification[a]		expected MW (Da)	possible isomers
A	7250.04 ± 0.48	8CAM	(8H)	7250.74	1
B	7499.68 ± 0.32	1G 7CAM	(1G7H)	7499.06	8
C	7134.44 ±0.28	1S 6CAM	(1S6H)	7134.74	28
D	7383.67 ± 0.81	1S 1G 5CAM	(1S1G5H)	7383.06	168
E	7018.80 ± 0.31	2S 4CAM	(2S4H)	7018.74	210
F	7267.18 ± 0.47	2S 1G 3CAM	(2S1G3H)	7267.06	840
L	6902.06 ± 0.39	3S 2CAM	(3S2H)	6902.74	420
M	7151.67 ± 0.38	3S 1G 1CAM	(3S1G1H)	7151.06	840
N	6785.68 ± 0.78	4S	(4S)	6786.74	105

[a] Abbreviations: CAM = carboxyamidomethyl groups; G = mixed disulfide with glutathione; S = intramolecular disulfide; H = free cysteine.

The ESMS spectrum of the aliquot withdrawn at time 0 shows the presence of a single component exhibiting a molecular mass of 7250.04 ± 0.48 Da which corresponds to the protein carrying eight carboxyamidomethyl groups (component A, 8H). Besides the reduced protein (A, 8H), the ESMS spectrum of the aliquot withdrawn after 1 min (Figure 2) reveals the simultaneous presence of four species. On the basis of their molecular masses, component B corresponds to a population of isomers containing one mixed disulfide with the exogenous glutathione and seven free SH groups (1G7H); C to intermediates containing one intramolecular disulfide bond and six free thiol groups (1S6H); D to species having one intramolecular disulfide bond, one mixed disulfide, and five free SH groups (1S1G5H); and E to species containing two intramolecular disulfide bonds and four free SH groups (2S4H). In addition to species E already observed, the analysis of the sample withdrawn at 60 min reveals the presence of species N containing four intra-

molecular disulfides (4S), L having three intramolecular disulfides and two free SH groups (3S2H), M containing three intramolecular disulfides, one mixed disulfide, and one free thiol group (3S1G1H), and F having two intramolecular disulfides, one mixed disulfide, and three free SH groups (2S1G3H). It should be noted that the fully reduced protein (A) and the three species B, C, and D detected at 1 min have already disappeared at this stage of the process. Finally, after 4 h of refolding, the ESMS spectrum shows essentially the presence of component N together with a very minor amount of species L.

In the use of ESMS, a further bonus is that each population of intermediates can be accurately quantified by measuring the total ion current produced by each species provided that the different components are endowed with comparable ionization capabilities (*12*, *13*). To control this point, a sample of reduced, denatured, and carboxyamidomethylated toxin α was mixed with an equal amount of oxidized protein. The concentration of both samples was determined spectrophotometrically at 280 nm using a molar extinction coefficient of 6490 M^{-1} cm^{-1}. This mixture was analyzed by ESMS, and the individual components were quantified by measuring the respective ion currents. Native toxin α constituted 52.3% of the mixture while the reduced, denatured, and carboxyamidomethylated protein accounted for the remaining 47.7%, demonstrating that oxidized and modified toxins yield similar ion currents. Therefore, the total ion current produced by each component in the refolding mixtures was used to calculate their relative abundance at different times of refolding.

The relative intensity of the disulfide bonded intermediates formed during the refolding process of natural toxin α is shown in Figure 3A. The fully reduced species (8H) rapidly disappears within the first 15 min, and the 3S2H intermediates predominate from the first minutes of refolding up to about 60 min when the fully oxidized species 4S becomes predominant. At 4 h the fully oxidized protein, species 4S, reaches 94%. These results do show that intermediates 3S2H tend to accumulate along the pathway and slowly interconvert into species 4S; the overall rate of refolding seems to depend therefore on the rate of conversion of intermediates 3S2H into species 4S. In addition, these analyses show that species containing mixed disulfide with glutathione do not accumulate to a concentration higher than 10% throughout the entire process, thus confirming that they constitute transient species which rapidly evolve toward the formation of intramolecular disulfide bonds. However, it was not possible to develop any quantitative analysis of the process because its complexity did not allow the calculation of any rate constants as previously made in the simpler case of RNase T1 (*13*).

Erabutoxin b (Eb) was reduced, denatured, and refolded in the same experimental conditions used for toxin α. The refolding pathway was then analyzed by the ESMS approach previously described. The relative percentages of the detected intermediates are reported in Figure 3B. No changes in the nature of disulfide bonded intermediates were observed in the refolding of Eb but they accumulate at different rates and to different extents. Species 3S2H are in fact predominant for almost the entire process, and at 4 h the yield of species 4S is much lower than that observed in the refolding of natural toxin α. Moreover, the 2S4H intermediates are

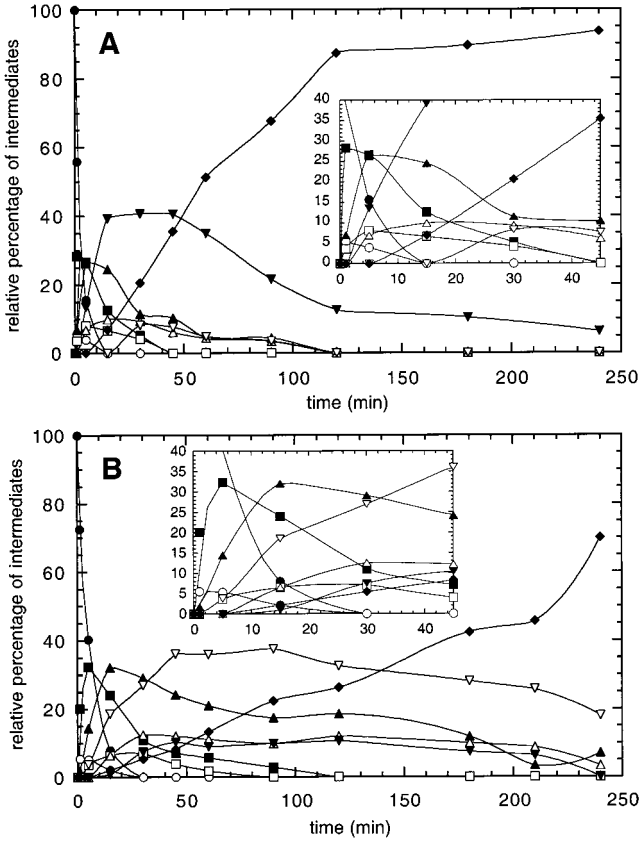

FIGURE 3: Time-course analysis of the refolding of natural toxin α (A) and erabutoxin b (B) in the presence of 3 mM GSH and 0.3 mM GSSG. The insets are zooms of the 45 min of refolding. Percentages of intermediates are derived by ESMS analysis as described in the text; 8H (●), 1G7H (○), 1S6H (■), 1S1G5H (□), 2S4H (▲), 2S1G3H (△), 3S2H (▼), 3S1G1H (▽), 4S (◆).

present in higher amounts and last longer than in the case of toxin α, and the two glutathione mixed disulfide species (2S1G3H and 3S1G1H) can be detected even at late refolding stages. Altogether these results might suggest that extensive forward and backward reactions, involving most intermediates, take place during the whole process.

Properties of the Synthetic Mutants of Toxin α. The synthetic toxins, α61 identical to natural toxin α, the deletion mutant α60, and the insertion mutant α62 (sequences are reported in Figure 1), were purified by HPLC and analyzed by ESMS. All the spectra show the presence of a single component exhibiting a molecular mass in excellent agreement with the expected mass values calculated on the basis of the amino acid sequences of individual toxins, as reported in Table 2. Further confirmation of the toxin sequences was brought by peptide mapping. The toxin samples were reduced, denatured, and alkylated as described, digested with trypsin, and then analyzed by direct MALDIMS. The recorded mass signals were associated with the corresponding tryptic fragments within the toxin sequences on the basis of their molecular mass and the specificity of the enzyme. The MALDI-mapping analyses demonstrate that the synthetic toxins have indeed the expected amino acid sequences (data not shown).

The synthetic toxins were incubated in the presence of the same GSH/GSSG redox buffer used for the natural toxins until complete oxidation, as monitored by HPLC. The oxidized toxins were purified and characterized for their

Table 2: Characterization of Toxins

	measured MW (Da)	expected MW (Da)	redox state	K_d ($\times 10^{-11}$ M)	reference
natural toxin α	6785.84 ± 0.88	6786.74	4 S-S	2.0 ± 0.6	(*28*)
α61	6794.23 ± 0.43	6794.80	8 SH	2.45 ± 0.60	this study
α60	6665.8 ± 0.39	6665.63	8 SH	2.35 ± 0.28	this study
α62	6882.26 ± 0.15	6881.82	8 SH	2.21 ± 0.38	this study
erabutoxin b	6859.03 ± 0.46	6859.75	4 S-S	7 ± 2	(*29*)

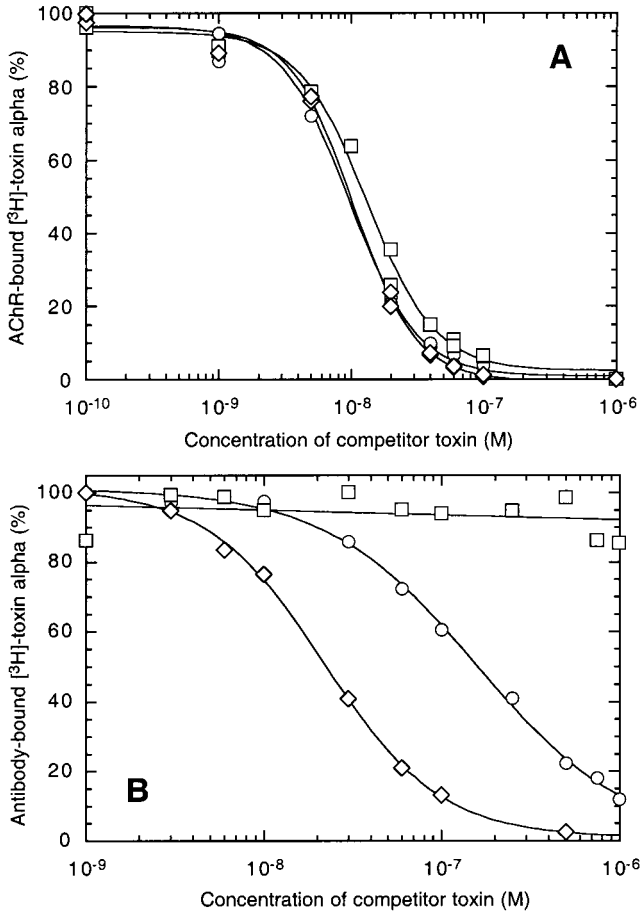

FIGURE 4: (A) Competition experiments between [^{3}H]-toxin α used as a radioactive tracer and various amounts of toxin mutants for binding to AChR from *Torpedo marmorata*. (B) Reactivity of the conformational antibody Mα-1 against toxin α variants. Analyses were carried by competitive radioimmuno-assay with [^{3}H]-toxin α. For both graphs: (○) α60; (◇) α61, (□) α62.

structural and biological properties. The analysis of the circular dichroism spectra for the three refolded synthetic toxins α60, α61, and α62, did not reveal any visible difference with the natural toxin α (data not shown). This suggests that the modifications introduced in the turn 2 have little influence on the overall tridimensional structure of the toxin. This was further confirmed by binding assays performed on the nicotinic acetylcholine receptor (AchR) and a conformational antibody (Mα-1). Both toxin mutants α60 and α62 bind to the AChR with an equilibrium dissociation constant (K_d) similar to the constant for α61 from which they originate as deduced from competition experiments (Figure 4A, Table 2). The modifications introduced in the turn 2 do not alter the toxin-binding capacity for the AChR. This result fits with previous findings by mutagenesis on erabutoxin Ea that the region involved in the receptor interface strictly corresponds to the bottom of the three loops (*5*).

Table 3: Half-Lives of Major Species Detected in the Refolding Analyses

	8H time (min)	4S time (min)
natural toxin α	2	60
synthetic toxin α	2	60
synthetic α60	0.5	35
synthetic α62	0.5	210
erabutoxin b	4	220

Boulain et al. (*19*) prepared a conformational monoclonal antibody specific for the region of the toxin modified in this study. Mapping of the Mα-1 epitope by chemical modification (*19*) or NMR analysis of amide hydrogen exchange (*23*) indicated that the recognition is spatially limited to the region involving Leu1-Nα and Lys15-Nϵ amino groups and the side chains of Asn5, Thr13, Lys15, and Lys58. Mα-1 does not recognize wild-type erabutoxin while deletion of Ser18 restored the binding of the antibody to erabutoxin Ea (*23*). Radioimmunoassays were carried out for the two mutants of toxin α, α62 and α60 (Figure 4B), and reproduced the expected pattern. Introduction of a serine at the position 18 in α62 as it exists in Eb completely abolished the binding to the antibody. Deletion of Glu20 in α60 has less drastic effects: binding is preserved although K_i is 100-fold lower (18.5 nM) than the value for wild-type (0.2 nM).

On the basis of these biochemical criteria, the synthetic α61 behaves exactly as natural toxin α; toxins α60 and α62 are foldable and reach a native-like structure except for the local structure of the turn 2 which mimics toxin A and Eb, respectively.

Refolding of Synthetic Mutants of Toxin α. α61 was reduced and denatured before starting the refolding experiments even if the ESMS analysis had shown it to be in the reduced state (Table 2). The ESMS analysis of the refolding process of α61 clearly shows that the same intermediates observed in the refolding of natural toxin α accumulate and that the distribution of these species is almost identical to that observed for the refolding of the natural protein (data not shown). Finally the two refolding processes seem to produce a fully oxidized species, 4S, at the same rate and with the same yield, as shown in Table 3. These results demonstrate that the synthetic toxin α61 is a perfect mimic of natural toxin α also regarding its refolding process. We then proceeded to the analysis of toxin mutants, α60 and α62.

α60 was reduced, denatured, and refolded in the presence of 3 mM GSH/0.3 mM GSSG, as described. The intermediates formed during the process were then analyzed and quantified by ESMS analysis (Figure 5A). The distribution of intermediates clearly shows that the fully reduced species disappears within the first 20 min, that species 3S2H is predominant only in the first 20 min, and that species 4S corresponding to the fully oxidized protein is predominant from 30 min onward (Table 3). As previously observed,

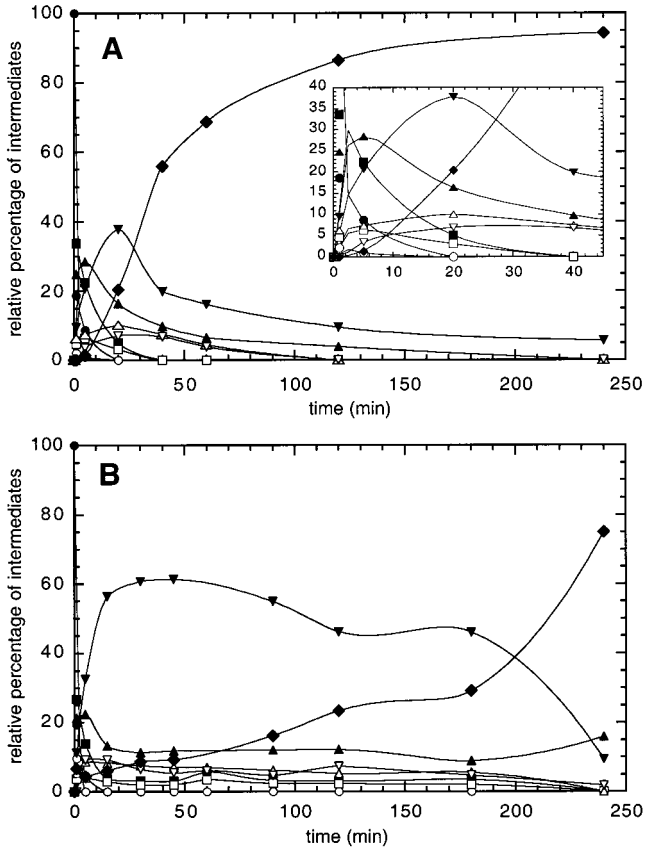

FIGURE 5: Time-course analysis of the refolding of α60 (A) and α62 (B) in the presence of 3 mM GSH and 0.3 mM GSSG. The insets are zooms of the 45 min of refolding. Percentages of intermediates are derived by ESMS analysis as described in the text; 8H (●), 1G7H (○), 1S6H (■), 1S1G5H (□), 2S4H (▲), 2S1G3H (△), 3S2H (▼), 3S1G1H (▽), 4S (◆).

intermediates containing mixed disulfides with glutathione accumulate only to a very low amount, thus confirming that they rapidly evolve toward the formation of intramolecular disulfides.

α62 was reduced, denatured, and refolded as described for the other toxins. There were no changes in the nature of disulfide containing intermediates of refolding, but they accumulated at different rates and at different levels (Figure 5B and Table 3). It is in fact clear that 3S2H intermediates predominate from the first minutes of refolding up to 3 h, thus indicating its slow tendency to be converted into the fully oxidized species. At 4 h species 4S accounted for about 75%, a value much lower than that observed in the refolding patterns of α61 and α60.

The appearance of species 4S in the refolding of synthetic toxins is reported in Figure 6, closed symbols, and Table 3. The results show very clearly that the appearance of 4S species proceeds faster in the refolding of α60 even at early stages, reaching the same final yield (95%) observed in the refolding of synthetic toxin α61. The comparison of the refolding of α61 and α60 confirms the difference previously observed between the refolding of toxin α and toxin A (*6*). The appearance of 4S species in the refolding of α62 is much slower than that observed in the refolding of α60 and α61, and it matches well with the appearance of 4S species of Eb (compare Figure 3B). This means that nothing except the length of turn 2 is responsible for the observed discrepancy between toxin α and Eb.

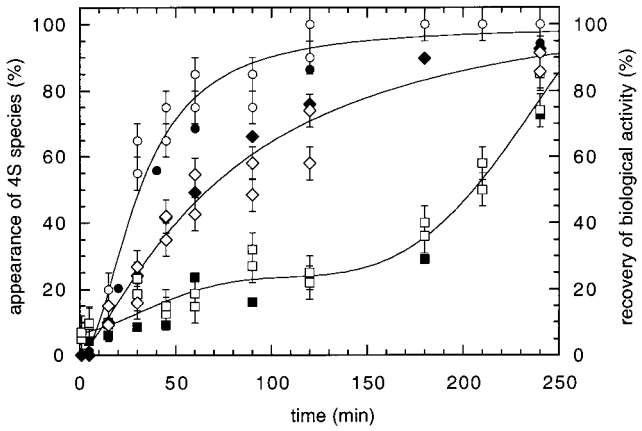

FIGURE 6: Closed symbols: appearance of 4S species in the toxin mutant refolding detected by ESMS analysis in the presence of 3 mM GSH and 0.3 mM GSSG. Open symbols: recovery of biological activity from aliquots of the same refolding reactions. The competition curves were used to determine the concentration of active toxin in each aliquot: (●/○) α60; (◆/◇) α61, (■/□) α62.

The intermediates identified by the ESMS analysis form a population of molecular species characterized by the same number of intramolecular disulfide bonds, mixed disulfides with glutathione, and free thiols. These intermediates may include nearly all possible disulfide bonded isomeric species. As the 4S species might in theory be constituted by as many as 105 isomeric species, the heterogeneity of all the 4S components was verified by measuring the percentage of toxins able to bind to the nicotinic acetylcholine receptor at various time points of refolding (Figure 6, open symbols). Unfolded or misfolded toxins indeed do not contribute to the biological activity as previously demonstrated by the comparison of the direct saturation curve and competition profile of [^{3}H]toxin α toward AChR (F. Bouet, personal communication). In all cases, the appearance of 4S species matched very well with the level of active protein, within the experimental error, demonstrating unambiguously that 4S is a unique native conformation containing the native set of disulfide bonds and that no isomerization occurs within the 4S species.

DISCUSSION

Previous studies of ellipticity recovery in the far UV had pointed out different refolding rates between toxin α and Eb (*6*). The possible determinants of the observed different rates of folding were assumed to arise from sequence variations in some secondary structure elements, particularly turn 2 which connects loops 1 and 2 (Figure 1) and varies from 3 to 5 residues in all known neurotoxins. We decided therefore to investigate the role of the length of turn 2 on the refolding process of snake toxins. To address this point, two mutants of toxin α, α62 and α60, were synthesized: mutant α62 has an insertion in turn 2 as observed in Eb (*2*), whereas α60 displays a deletion in this turn. Turn 2 seems to have no role in the stability of the native toxin and may just have a role in the kinetics of the refolding process. The thermodynamic stability of α, α60, α62, and Eb was in fact investigated by thermal denaturation followed by CD showing a very similar T_m for α, α60, and α62, while Eb is less stable by about 15 °C (Robert Thai, personal communication).

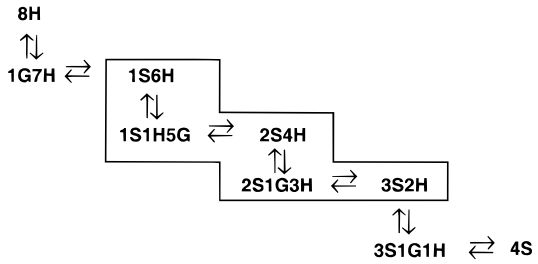

FIGURE 7: The sequential pathway of folding used by natural toxin α and variants. The box surrounds all the intermediates accumulating during the folding.

The results presented in this paper demonstrate that indeed the length of turn 2 affects the folding rate in toxins and can be summarized in a few words: the shorter the turn, the faster the folding. A near 2-fold increase in the refolding rate, in fact, can be obtained by shortening turn 2, but the most spectacular observation is the effect of inserting a serine residue in the turn 2 which decreases the refolding rate by a factor of 3.5. The extent of the variation in the refolding rates observed for synthetic toxins α fit remarkably well with that measured for the corresponding natural toxins. Synthetic toxin α62 and Eb, which share the same length of turn 2, show an almost identical refolding rate and pathway, despite the numerous amino acid substitutions. Turn 2 appears therefore to be the main determinant for the differences observed in the refolding rate of toxins α. These results might suggest that the length of a particular turn might control the overall refolding rate of three-fingered proteins.

All natural and synthetic toxins do refold according to the sequential pathway established formerly for RNases T1 and A (*12*, *13*) as shown in Figure 7. The refolding of all these proteins occurs via reiteration of two sequential steps: (i) formation of a mixed disulfide with glutathione, and (ii) internal attack of a free SH group to form an intramolecular disulfide bond. This sequential pathway seems to be a general mechanism for single-domain disulfide-containing proteins as it has been observed before, despite differences in the experimental conditions used for the refolding experiments, such as the ratio of GSH/GSSG and the presence of folding factors. This mechanism predicts that only a limited number of intermediates is formed in the process as compared to all those theoretically possible. In particular, no population of intermediates containing more than one mixed disulfide with glutathione was detected in all the folding processes analyzed. These observations allowed us to exclude some possible refolding pathways, thus significantly decreasing the number of paths. However, within the frame of this general pathway, differences exist in the amount and accumulation rate of individual intermediates arising from the peculiar protein under investigation. When the refolding pathways of RNase A and toxin α, both containing four disulfide bonds, are compared, some differences can be detected. 2S4H intermediates predominate along the RNase A refolding (*11*, *12*), while the 3S2H intermediates represent the most abundant species in the case of toxin α. This predominance suggests that refolding of toxin α could be driven by statistical pairing of cysteine residues (see Table 1 for the number of isomers) without the restrictions due to the early acquisition of secondary structure elements reported for RNase A (*24*).

A statistical mechanism of disulfide bond formation implies that a large number of cysteines have to be brought close to each other in the right orientation during the refolding process. A lower degree of conformational freedom in the polypeptide chain will result in a lower number of possible cysteine pairings which leads to the formation of a lower number of disulfide intermediates. The variable β-turn propensity of turn 2 is likely to be a major early determinant in this process. A short turn, CPG, as found in toxin A and α60, reduces more dramatically the folding space than the longer turn, CSPGE, that is found in Eb or α62. If disulfide bond formation proceeds randomly, the result of increasing the local flexibility will be a higher probability of formation of non-native intermediates. Analyses by isoelectric focusing of the number of possible isomers formed during the folding of natural toxin A, toxin α, and Eb (F. Bouet, personal communication) showed that, indeed, the number of intermediates is proportional to the length of turn 2. Thus, the early reduction in the number of possible disulfide intermediates benefits directly the folding rate.

Refolding of toxin under study eventually leads to the formation of a unique 4S species that contains only native bonds. Once the correct disulfide bonding is reached, the final β-sheets organization might occur within milliseconds by hydrophobic collapse, as exemplified in a recent study on the refolding of oxidized CTX III, a 60 amino acid cardiotoxin from *Naja naja atra* (*25*). Consequently, formation of the 4S species goes through an obligatory transient 3S2H intermediate with native bonds. Whether this intermediate is unique cannot be experimentally addressed yet. A more detailed structural characterization of the 3S2H intermediates present in the refolding of toxins is currently in progress to define this point. Several isomerization reactions of the 3S2H population are needed to generate a native 3S2H structure. The occurrence of isomerization reactions of the 3S2H population is supported by the analysis of the refolding pathways of Eb (Figure 3B) and α62 (Figure 5B) in which the intermediates 1S6H and 2S4H and the glutathione mixed disulfide species 1S1G5H, 2S1G3H, and 3S1G1H accumulate and last longer throughout the refolding process. These data suggest the occurrence of an equilibrium among these species in which backward reactions could then occur up to the 1S6H species to rescue kinetically trapped non-native intermediates. The isomerization equilibrium involving different species might confidently be applied also to the faster refolding processes of toxin α and α60 as shown by the accumulation of intermediates other than the 3S2H species at the early refolding stages (see insert in Figure 3A and 5A). Altogether, these rescue reactions seem to kinetically control the refolding of toxins. In this respect, the role of turn 2 in controlling the folding kinetics can be explained in that the conformational freedom of this segment heavily affects the backward and forward rescue reactions.

Alternatively, formation of the fourth disulfide bond might itself be a quite slow reaction, due to steric constraints associated with forming the buried disulfides, as seen in some steps in the BPTI refolding pathway (*26*). This slow interconversion should cause the occurrence of intramolecular isomerization within the 3S2H population which should eventually work as a kinetic trap. However, this latter interpretation does not explain the accumulation of intermediates other than 3S2H up to the later stages in the process

of the slow folding toxins.

In vivo folding of snake toxins probably uses a pathway similar to that observed in vitro. Assuming that a kinetic competition exists between productive folding processes and aggregation propensity (*27*), we suggest that, from a biotechnology perspective, any gain in the folding rate can benefit the production yield of recombinant proteins. Our work provides an original way to improve yields of recombinant protein by turns engineering.

ACKNOWLEDGMENT

We are grateful to Dr. Gilles Mourier and Ghislaine Henneke for their help in peptide synthesis and purification, Dr. Denis Servent for the bioassays, and Suzanne Pinkasfeld for the gift of snake venom toxins.

REFERENCES

1. Harrison, P. M., and Sternberg, M. J. E. (1996) *J. Mol. Biol. 264*, 603−623.
2. Ohno, M., Ménez, R., Ogawa, T., Danse, J. M., Shimohigashi, Y., Fromen, C., Ducancel, F., Zinn-Justin, S., Le Du, M.-H., Boulain, J.-C., Tamiya, T., and Ménez, A. (1997) *Prog. Nucleic Acid Res. Mol. Biol. 59*, 307−363.
3. Kieffer, B., Driscoll, P. C., Campbell, I. D., Willis, A. C., van der Merve, P. A., and Davis, S. J. (1994) *Biochemistry 33*, 4471−4482.
4. Flechter, C. M., Harrison, R. A., Lachman, P. J., and Neuhaus, D. (1994) *Structure 2*, 185−199.
5. Tremeau, O., Lemaire, C., Drevet, P., Pinkasfeld, S., Ducancel, F., Boulain, J. C., and Ménez, A. (1995) *J. Biol. Chem. 270*, 9362−9.
6. Ménez, A., Bouet, F., Guschlbauer, W., and Fromageot, P. (1980) *Biochemistry 19*, 4166−4172.
7. Wu, C.-Y., Chen, W.-C., Ho, C.-L., Chen, S.-T., and Wang, K.-T. (1997) *Biochem. Biophys. Res. Commun. 233*, 713−716.
8. Fromen-Romano, C., Maillère, B., Drevet, P., Lajeunesse, E., Ducancel, F., Boulain, J. C., and Ménez, A. (1997) *Protein Eng. 10*, 101−108.
9. Ricciardi-Boti, A., Khayati, M., Dajas, F., Boulain, J., Ducancel, F., and Ménez, A. (1998) (submitted for publication).
10. Miranker, A., Robinson, C. V., Radford, S. E., Aplin, R. T., and Dobson, C. M. (1993) *Science 262*, 896−899.
11. Torella, C., Ruoppolo, M., Marino, G., and Pucci, P. (1994) *FEBS Lett. 352*, 301−306.
12. Ruoppolo, M., Lundström-Ljung, L., Talamo, F., Pucci, P., and Marino, G. (1997) *Biochemistry 36*, 12259−12266.
13. Ruoppolo, M., Freedman, R. B., Pucci, P., and Marino, G. (1996) *Biochemistry 35*, 13636−13646.
14. Eaker, D., and Porath, J. (1967) *Jpn. J. Microbiol. 11*, 353−355.
15. Ménez, A., Morgat, J. L., Fromageot, P., Ronseray, A. M., Boquet, P., and Changeux, J. P. (1971) *FEBS Lett. 17*, 333−335.
16. Charpentier, I., Pillet, L., Karlsson, E., Couderc, J., and Ménez, A. (1990) *J. Mol. Recognit. 3*, 74−81.
17. Sato, S., and Tamiya, N. (1971) *Biochem. J. 122*, 453−461.
18. Gray, W. R. (1993) *Protein Sci. 2*, 1732−1748.
19. Boulain, J.-C., Ménez, A., Couderc, J., Faure, G., Liacopoulos, P., and Fromageot, P. (1982) *Biochemistry 21*, 2910−2915.
20. Sobel, A., Weber, M., and Changeux, J.-P. (1977) *Eur. J. Biochem. 80*, 215−224.
21. Cheng, Y., and Prusoff, S. (1973) *Biochem. Pharmacol. 22*, 3099−3108.
22. Hwang, C., Sinskey, A., and Lodish, H. (1992) *Science 257*, 1496−1502.
23. Zinn-Justin, S., Pillet, L., Ducancel, F., Thomas, A., Smith, J. C., Boulain, J.-C., and Ménez, A. (1994) *Protein Eng. 7*, 917−923.
24. Lustig, B., and Fink, A. L. (1992) *Biochim. Biophys. Acta 1121*, 229−233.
25. Sivaraman, T., Kumar, T. K. S., Chang, D. K., Lin, W. Y., and Yu, C. (1998) *J. Biol. Chem. 273*, 10181−10189
26. Zhang, J.-X., and Goldenberg, D. P. (1993) *Biochemistry 32*, 14075−14081.
27. Orsini, G., and Goldberg, M. (1978) *J. Biol. Chem. 253*, 3453−3458.
28. Weber, W., and Changeux, J. P. (1974) *Mol. Pharmacol. 10*, 1−14.
29. Pillet, L., Tremeau, O., Ducancel, F., Drevet, P., Zinn-Justin, S., Pinkasfeld, S., Boulain, J.-C., and Ménez, A. (1993) *J. Biol. Chem. 268*, 909−916.
30. Kraulis, P. (1991) *J. Appl. Crystallogr. 24*, 946−950.

BI981492J